Establishing a molecular relationship between chondritic and cometary organic solids

George D. Cody[a,1], **Emily Heying**[a], **Conel M. O. Alexander**[b], **Larry R. Nittler**[b], **A. L. David Kilcoyne**[c], **Scott A. Sandford**[d], **and Rhonda M. Stroud**[e]

[a]Geophysical Laboratory, Carnegie Institution of Washington, 5251 Broad Branch Road NW, Washington, DC 20015; [b]Department of Terrestrial Magnetism, Carnegie Institution of Washington, 5241 Broad Branch Road NW, Washington, DC 20015; [c]Advanced Light Source, Lawrence Berkeley Laboratory, Berkeley, CA 94720; [d]Astrophysics Branch, Mail Stop 245-6, National Aeronautics and Space Administration Ames Research Center, Moffet Field, CA 94035; and [e]Naval Research Laboratory, Washington, DC 20015

Edited* by Mark H. Thiemens, University of California, La Jolla, CA, and approved February 25, 2011 (received for review October 25, 2010)

Multidimensional solid-state NMR spectroscopy is used to refine the identification and abundance determination of functional groups in insoluble organic matter (IOM) isolated from a carbonaceous chondrite (Murchison, CM2). It is shown that IOM is composed primarily of highly substituted single ring aromatics, substituted furan/pyran moieties, highly branched oxygenated aliphatics, and carbonyl groups. A pathway for producing an IOM-like molecular structure through formaldehyde polymerization is proposed and tested experimentally. Solid-state ^{13}C NMR analysis of aqueously altered formaldehyde polymer reveals considerable similarity with chondritic IOM. Carbon X-ray absorption near edge structure spectroscopy of formaldehyde polymer reveals the presence of similar functional groups across certain Comet 81P/Wild 2 organic solids, interplanetary dust particles, and primitive IOM. Variation in functional group concentration amongst these extraterrestrial materials is understood to be a result of various degrees of processing in the parent bodies, in space, during atmospheric entry, etc. These results support the hypothesis that chondritic IOM and cometary refractory organic solids are related chemically and likely were derived from formaldehyde polymer. The fine-scale morphology of formaldehyde polymer produced in the experiment reveals abundant nanospherules that are similar in size and shape to organic nanoglobules that are ubiquitous in primitive chondrites.

The predominant form of organic matter in primitive solar system bodies [e.g., primitive asteroids, interplanetary dust particles (IDPs) and comets] exists as a refractory (or a recalcitrant) solid phase. Primitive chondritic meteorites (petrologic type 1 and 2) contain up to 2 wt. % of chemically complex and refractory organic solids that is commonly referred to as insoluble organic matter (IOM) (1). IOM is the predominant form of organic carbon present in meteorites, in all cases far exceeding the total suite of soluble organics. The abundance of organic solids in IDPs, both anhydrous and hydrous types, is much higher up to 44 atomic % (2). The abundance of refractory organic solids in comets is estimated to be 23 wt % (3).

Whereas studies of solar system refractory organic solids are extensive, there is no consensus regarding their point of origin, nor their mode of synthesis. A contributing factor to this problem is that there are many different regions in the Galaxy where extensive organosynthesis occurs. For example, it is has been proposed that refractory organics contained within comets and IDPs formed as a consequence of low-temperature UV-induced photo polymerization of small organic molecules condensed onto ice mantles of silicate grains in the interstellar medium (ISM) (4–6). It is also known that extensive complex organic synthesis also occurs in the circumstellar envelopes of highly evolved stars (7). If such organic matter survives processing in the ISM and is incorporated into star forming molecular clouds, then it appears reasonable to presume that these organics would also be present as constituents in primitive solar system bodies (8). The detection of IR emission from UV excited polycyclic aromatic hydrocarbons (PAHs) in protoplanetary disks certainly raises the expectation that PAHs could be components of organic solids in primitive solar system bodies (9).

Other proposals consider the synthesis of refractory organics in primitive bodies to have occurred within the inner protoplanetary disk at relatively high temperatures. For example, an early hypothesis suggested that organic solids formed through gas phase and gas-grain reactions involving methane $+ N_2$ (10). Later, Fischer Tropsch-like reactions involving $CO + H_2$ over clay minerals at $T \leq 873$ K were proposed to be a source of IOM (11). More recently, Llorca and Casanova (12) performed experiments where reaction of CO/H_2 gas over kamacite particles ($T = 473$ K) yielded low molecular weight organic compounds and amorphous carbonaceous deposits on the particles leading them to conclude that such processes could explain the presence of organic solids in carbonaceous chondrites. Nuth et al. (13) have performed similar experiments at higher temperatures and observed continuous growth of carbonaceous coatings on grains leading them to propose that such carbonaceous solids would be readily incorporated into accreting asteroids and could be carried outward to the comet forming regions of the solar system (13).

Acetylene condensation reactions (i.e., soot chemistry) at temperatures in the range of 900 to 1,100 K have also been proposed as a plausible inner solar system origin of IOM (14). Alternatively, it has been proposed that organic solids formed in plasmas close (approximately 1 AU) to the young sun (15) and may have been incorporated into asteroids. Given the apparent ease of radial transport from within the solar system outward along the midplane early in solar system history (16), it appears that synthesis scenarios may not be constrained by radial distance from the sun.

Given multiple sources of organics in various regions of the galaxy, both hot and cold, and the apparent extensive radial mixing that occurred in the early solar system (16), there are few astronomical constraints either for a point of origin nor the mode of synthesis of refractory organic solids present in primitive solar system bodies. Indeed, as both hot and cold origins of refractory organic solids are theoretically plausible, it is possible that there is no chemical relationship between refractory organic solids in comets, IDPs, and chondritic IOM. The most robust constraints for the origin of organic solids in comets, IDPs, and primitive chondrites must, therefore, come from direct studies of the primitive organic solids themselves. For example, it has been shown that primitive IOM from petrologic type 1 and 2 carbonaceous chondrites must have accreted cold and was never subjected to sustained temperatures in excess of approximately 100 °C (17).

Author contributions: G.D.C. designed research; G.D.C., E.H., C.M.A., L.R.N., A.L.D.K., and R.M.S. performed research; G.D.C., C.M.A., L.R.N., A.L.D.K., S.A.S., and R.M.S. analyzed data; and G.D.C. wrote the paper.

The authors declare no conflict of interest.

*This Direct Submission article had a prearranged editor.

[1]To whom correspondence should be addressed. E-mail: gcody@ciw.edu.

This article contains supporting information online at www.pnas.org/lookup/suppl/doi:10.1073/pnas.1015913108/-/DCSupplemental.

This result rules out any high temperature origins-scenario for IOM in primitive chondrites.

In this paper we apply advanced ^{13}C solid-state NMR and carbon (1*s*) X-ray absorption near edge structure (C-XANES) spectroscopy to show that the molecular spectroscopic characteristics of primitive solar system organic solids in carbonaceous chondritic meteorites, IDPs, and Comet 81P/Wild 2 particles are consistent with a common low-temperature origin. We demonstrate via experiment that a formaldehyde-derived polymer may be a viable point of origin for organic solids in primitive solar system bodies.

Results and Discussion

Refining the Molecular Structure of Primitive IOM. Solid-state ^{13}C NMR remains one of the most powerful analytical techniques available for obtaining molecular structural information on chondritic IOM. The most striking aspect of solid-state ^{13}C NMR spectra of primitive IOM is the chemical complexity indicated by the extremely broad spectral features (18–20). Notwithstanding this complexity applying multiple independent and complementary ^{1}H and ^{13}C NMR experiments provides a self-consistent generalized structure for primitive IOM (21, 22). For example, in the case of Murchison (a type 2 CM chondrite) IOM *ca.* 30% of the carbon exists in the *sp*^{3} electronic configuration, of which *ca.* 40% of the *sp*^{3} carbon is oxygenated (i.e., alcohol and/or ether) and the remainder is methyl, methylene, and methine. The *ca.* 70% *sp*^{2} bonded carbon exists predominantly in the form of olefinic and/or aromatic moieties (at *ca.* 60% of the total carbon) and carbonyl (both ketone and carboxyl) at *ca.* 10% of the total carbon. Combining the results of multiple independent NMR experiments has revealed that aromatic carbon in Murchison's IOM consists of small molecules (1–2 ring) that are very highly substituted and the saturated (*sp*^{3}) carbon exists in highly branched structures (20, 21). Comprehensive NMR studies of IOM from other type 1 and & 2 chondrites from different groups (e.g., CR, CI, and Tagish Lake) revealed significant variation in the proportion of *sp*^{2} and *sp*^{3} bonded carbon, but in all cases aromatic moieties are small and very highly substituted and the saturated carbon is highly branched. Significantly, none of the solid-state NMR analyses indicated the presence of abundant highly condensed PAHs) in IOM. Large PAHs, so prevalent throughout the galaxy (8), evidently do not contribute significantly to the inventory of organic solids in primitive chondrites.

Notwithstanding the success of standard NMR experiments, there is the potential to extract additional information through the application of more complex multidimensional NMR experiments. It is worth recalling that an essential attribute of all high-resolution solid-state NMR experiments of amorphous organic solids is the implementation of magic angle sample spinning (MAS), wherein the solid sample is physically spun at an angle of 54.7° relative to the static magnetic field. Fast MAS serves to average the severe spectral broadening derived from (among a number of effects) the random orientation of chemical bonds relative to the static magnetic field. Variation in resonance frequency of a given nucleus in a given bond with orientation relative to the static magnetic field is described by the chemical shielding tensor (a rank 2 tensor) that is fixed in the bond's reference frame and is extremely sensitive to the electronic structure and symmetry of the bond. Fast MAS averages the chemical shielding tensor to a single (isotropic) value yielding simplified spectra, rendering the symmetry and anisotropic characteristics of the individual chemical shielding tensors unrecoverable. This is, in some cases, unfortunate as some carbon nuclei in different electronic environments (hence having different chemical shielding tensors) have nearly identical isotropic chemical shifts. For example, both substituted aromatic carbon and condensed aromatic carbon exhibit an isotropic shift (δ_{iso}) at *ca.* 130 ppm (22). These two aromatic carbon types do, however, have different chemical shielding tensors and can be distinguished from each other by their significantly different chemical shielding powder patterns if analyzed without MAS (22).

The two-dimensional magic angle turning (MAT) experiment (23) was designed to separate individual powder patterns (in the MAS dimension, ω_2) along a high-resolution isotropic NMR spectrum (in the evolution dimension, ω_1). In the present case, the 2D MAT experiment was optimized using vanillic acid powder as a standard prior to analyzing high purity IOM derived from the Murchison meteorite (*SI Text*). The 2D MAT spectrum of Murchison IOM is presented in Fig. 1*A*. The spectral contour plot reveals the manifolds of *sp*^{3} and *sp*^{2} carbon and the distinct differences in their shielding anisotropy (Fig. 1*A*). The summed projection onto the evolution dimension (Fig. 1*B*) reveals that the MAT experiment succeeds in yielding a high quality isotropic spectrum as compared to that obtained using conventional 1D ^{1}H-^{13}C cross-polarization MAS NMR at high sample spinning frequency ($\omega_r/2\pi = 12$ kHz).

Slices of the MAT spectra of vanillic acid taken along the evolution dimension yield well resolved static (powder) patterns (e.g., in Fig. 2 *A* and *B*) for aromatic C-H and aryl-O (δ_{iso} at 118 and 142 ppm, respectively) that record the symmetry and anisotropy typical of chemical shielding tensors for such functional groups (22). Extracted powder patterns for Murchison are less distinct as compared with vanillic acid due to the inherent chemical complexity of IOM. Nevertheless, a single tensor fit (Fig. 2*C*) of the powder pattern for $\delta_{\mathrm{iso}} = 130$ ppm corresponds well to that expected for substituted aromatic carbon (22) and is distinguishable from the expected powder pattern for condensed aromatic carbon that also has δ_{iso} ca. 130 ppm (Fig. 2*E*). Note that each fitted powder pattern is constrained by the requirement that $\delta_{\mathrm{iso}} = 1/3(\delta_{11} + \delta_{22} + \delta_{33})$, where δ_{ii} are the principal axis values of the diagonalized chemical shielding tensor.

The fact that aromatic carbon in chondritic IOM is in the form of small substituted aromatic molecules is already known (20, 21). The 2D-MAT experiment does, however, provide the following structural refinement. In the studies of Hayatsu et al. (24) an abundance of various alkyl phenols were detected following reaction of IOM with CuO in a hot, strongly basic, solution. Hayatsu et al. (24) concluded from this observation that the chondritic IOM polymer likely had a predominance of alkyl aryl ether linkages. If this is correct, then evidence of abundant aryl-O

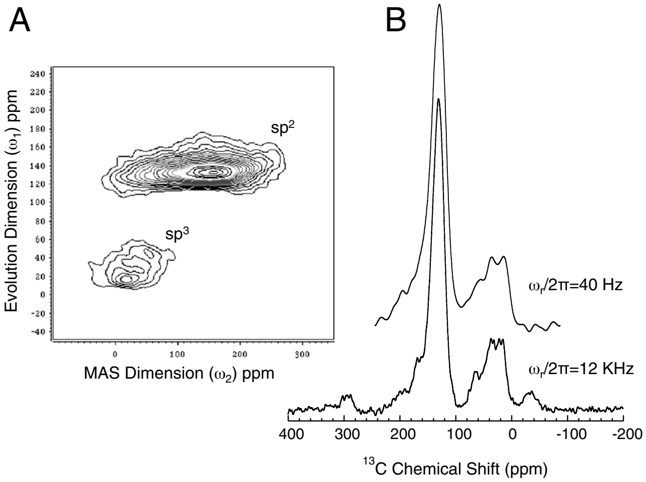

Fig. 1. (*A*) A 2D ^{13}C NMR contour plot of Murchison IOM obtained via the MAT experiment that separates isotopic (along the evolution dimension) from anisotropic chemical shifts (along the MAS dimension), regions corresponding to *sp*^{3} and *sp*^{2} hydridized carbon are indicated. (*B*) Projection of the 2D NMR MAT ($\omega_r/2\pi = 40$ Hz) data in the evolution dimension yields the ^{13}C CPMAS isotropic spectrum of Murchison that is identical to a standard 1D ^{13}C CPMAS spectrum ($\omega_r/2\pi = 12$ Khz).

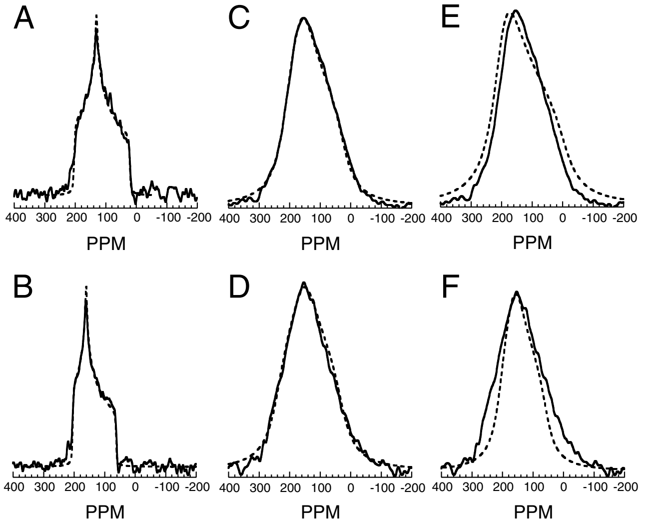

Fig. 2. Extracted chemical shielding powder pattern spectra obtained via the MAT experiment. Each powder pattern is fit to yield the isotropic shift δ_{iso}, the asymmetry parameter, η (where $0 \geq \eta \geq 1$), and the reduced anisotropy, d ($\square = \delta_{iso} - \delta_{ZZ}$), from which the PAS chemical shift tensor values, δ_{11} δ_{22}, and δ_{33}, may be determined. The fits are constrained by the requirement that δ_{iso} $(\omega_1) = 1/3(\delta_{11} + \delta_{22} + \delta_{33})$ (ω_2). For the vanillic acid standard, (*A*) presents the extracted powder pattern for aromatic C-H fit with $\delta_{iso} = 118$ ppm, $\eta = 0.75$, and $d = -97$ ppm; (*B*) presents the extracted powder pattern of aryl-OH fit with $\delta_{iso} = 142$ ppm, $\eta = 0.55$, and $d = -80$ ppm; both sets of fit parameters are typical for these functional groups. The extracted powder patterns for Murchison exhibit considerable inhomogeneous broadening, (*C* and *D*). Extraction and fitting of the powder pattern of the central aromatic peak at 130 ppm, (*C*), yields a good fit to a single shielding tensor with $\delta_{iso} = 130$ ppm, $\eta = 0.5$, and $d = -105$ ppm, consistent with substituted aromatic carbon (18), note that in (*E*), the extracted 130 ppm powder pattern average powder pattern for Murchison IOM differs considerably from condensed aromatic carbon (18). The extracted powder pattern at 142 ppm, (*D*) is fit to a single shielding tensor with $\delta_{iso} = 142$ ppm, $\eta = 0.8$, and $d = -108$ ppm. Note that is powder pattern's reduced anisotropy and symmetry differs completely from that of aryl-O, (*F*).

should be observed via solid-state ^{13}C NMR. One-dimensional NMR cannot unambiguously distinguish aryl-O carbon from nonaromatic enols. Thus, it is particularly significant that in the 2D-MAT NMR spectrum, the fit of the extracted powder pattern of Murchison IOM at $\delta_{iso} = 142$ ppm (Fig. 2*D*) does not correspond to what is expected for aryl carbon bonded to oxygen (22); rather, the best fit tensor exhibits considerably less radial symmetry and much greater anisotropy consistent with furan and/or pyran moieties (Fig. 2*F*).

Integrating these results with previously obtained molecular structural data from NMR studies (20, 21) reveals a molecular structure of Murchison IOM composed of approximately 30% highly branched aliphatics and alcohols, ≤25% furanic/pyranic moieties, ≥35% highly substituted single ring aromatics and olefins, and approximately 10% carboxyl and ketone; all linked together in a complex insoluble polymer. Note that only a generalized description of IOM is possible, attempting to construct a visual molecular representation of IOM is futile given the enormous chemical variation evident in the widths of the peaks for each functional group class.

Given the constraint of a low-temperature origin for chondritic IOM (17), there are few organic reaction mechanisms that could give rise to such a complex macromolecule. The presence of abundant furan, in particular, provides a clue as to the origin of chondritic IOM. Substituted furans form readily from polyalcohols through dehydration and intramolecular cyclization (25) (reaction 3, Fig. 3). Cooper et al. (26) identified polyhydroxylated molecules (e.g., sugars and sugar derivitives) in an aqueous extract of the Murchison meteorite and speculated that the IOM might be derived from the condensation of sugar-like molecules. Such a scenario is consistent with the macromolecular structure of IOM as determined by solid-state NMR.

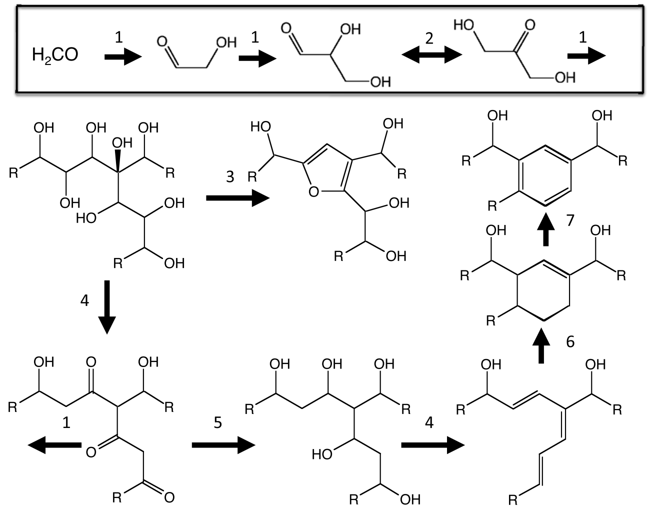

Fig. 3. Schematic representation of reactions that lead from formaldehyde to formaldehyde polymer. Hydrogen atoms bonded to carbon are excluded for clarity. Single and double bonds are designated with single and double lines, respectively. Formaldehyde condenses with itself (reaction 1) to form glycoaldehyde. Sequential Aldol condensations yield polyalcohols. Intramolecular hydride transfer (reaction 2) intraconverts glyceraldehdye to dihydroxy acetone. Aldol condensation (reaction 1) with dihydroxyacetone lead to branched polyalcohols. Polyalcohols may eliminate H_2O and cyclize forming furan moieties (reaction 3). Dehydration of branched polyalcohol (reaction 4) yields polyketone that may condense further via Aldol condensation (reaction 1) or through successive reduction and elimination reactions (reactions 5 and 4) yield poly-olefin that may undergo either inter- or intramolecular cycloaddition reactions to form cyclohexene moieties via reaction 6. Dehydrogenation (reaction 7) yields highly substituted aromatic moieties.

Cooper et al. (26) considered that the most likely source of polyalcohols in primitive chondrites was from the formose condensation reaction (reaction 1, Fig. 3); wherein starting with formaldehyde successive condensations lead to glycolaldehdye, glyceraldehyde, etc. Intramolecular hydride transfer (reaction 2, Fig. 3) (e.g., interconverting glyceraldehyde into dihydroxy acetone) leads to the possibility of forming branched polyalcohols. A highly branched polyalcohol polymer provides also provides a straightforward means for the low-temperature formation of small highly substituted aromatics that are abundant in primitive chondritic IOM (20, 21). Successive water elimination-hydride transfer reductions will lead to the formation of polyolefin (reactions 4 and 5, Fig. 3). Inter- or intramolecular cycloaddition reactions (25) would provide a facile route for the formation of small highly substituted aromatic molecules as outlined schematically in reactions 4–7, Fig. 3. Reactions 2 and 6 lead to the potential of a high degree of polymeric cross-linking, a defining characteristic of IOM.

Comparison of Formaldehyde-Derived Polymer with Chondritic IOM. Formaldehyde is seen in the gas phase in many interstellar environments (27) and cometary comae (28). It is also one of the main products formed when CH_3OH containing ices are exposed to ionizing radiation in the form of UV photons or high-energy ions (4, 6). Methanol is a major component of many interstellar, protosolar, and cometary ices (29, 30). Furthermore, laboratory studies of H_2CO in ices of mixed compositions has demonstrated that this material can polymerize in situ during the warm up of the ices, with polymerization of the ices beginning at temperatures as low as 40 K (31).

The outcome of formaldehyde polymerization in this study is the formation of a solid precipitate that forms within hours (*SI*

Text). To explore whether formaldehyde-derived solids bear any similarity in molecular structure to chondritic IOM, insoluble formose solids were subjected to solid-state NMR analysis. Analysis of the 1D variable amplitude cross-polarization (^{1}H-^{13}C) NMR spectra (Fig. 4) of the formaldehyde polymer (as synthesized, designated F50; *SI Text*) and after being heated in water suggests that formaldehyde condensation reactions could be a primary source of chondritic IOM. The formose polymer synthesized at 50 °C (F50) exhibits a complex molecular structure composed of abundant methyl (20 ppm), methine (37 ppm), alcohols (80 ppm), olefins (129 ppm), furan (143 ppm), carboxyl (175 ppm), and ketone (204 ppm). The relatively abundant methine and olefinic carbon (Fig. 4) is consistent with cycloaddition reactions (reaction 6, Fig. 3) being integral to the formation of the insoluble formaldehyde polymer. It is clear that the (as synthesized) formaldehyde polymer (F50, Fig. 4) contains considerably more saturated functional groups than the IOM isolated from the Murchison (CM2) chondritic meteorite (Fig. 4).

Progressive heating in water transforms the formaldehyde-derived solids into a macromolecule that bears considerable similarity to Murchison IOM (Fig. 4). The principal changes in molecular structure associated with progressive heating in water involves the dehydrogenation of cycloaddition-derived cyclohexene moieties to yield highly substituted single ring aromatic moieties (e.g., path 7, Fig. 3), evident by the loss of methine intensity (37 ppm) and the development of intensity at 130 ppm (Fig. 4) and dehydration of alcohols evident by a loss of intensity at 80 ppm.

The most significant difference between the F250 and Murchison IOM molecular structures is that the later has proportionally more alcohol and the F250 residue has proportionally more carboxyl and ketone. Reduction of some of the oxygenated *sp*^{2} carbon in F250 to alcohol is not a difficult reaction and would yield an organic solid very similar to that of Murchison IOM. It should be noted that while heating at 250 °C transformed the formaldehyde polymer into an organic solid similar in structure to Murchison IOM, this does not require that Murchison IOM was also subjected to such high temperatures, longer time at more moderate temperatures (e.g., many years at approximately 100 °C) would likely yield the same result. Murchison IOM's molecular structure is, therefore, consistent with a formaldehyde polymer origin, but with chemical modification likely arising from low-temperature parent body processing.

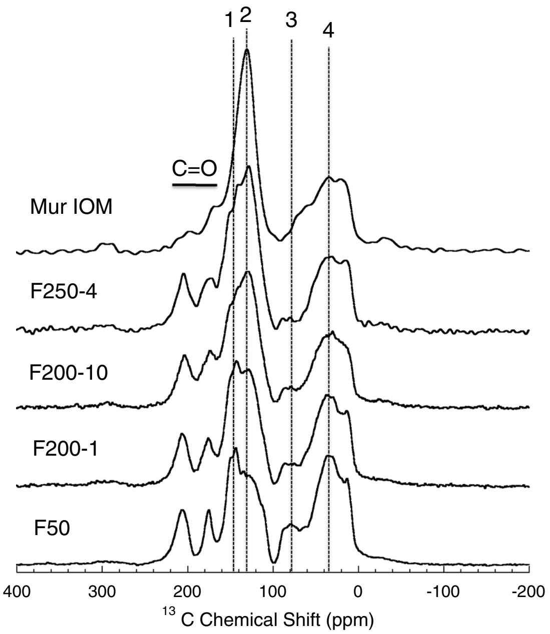

Fig. 4. (*A*) ^{13}C CPMAS NMR spectra of the as synthesized formose polymer (F50), formose polymer heated in water at 200 °C for one hour (F200-1), 200 ° C for 10 hours (F200-10), and 250 °C for 4 hours (F250-4), and Murchison IOM. The primary transformation upon heating is the conversion of methine carbon (peak 4 at 37 ppm) to aromatic/olefinic carbon (peak 2 at 130 ppm) through dehydrogenation and the dehydration of alcohols (peak 3 at 80 ppm) also to olefinic carbon (peak 2 at 130 ppm). The prominent enol peak (peak 1 at 145 ppm) progressively becomes hidden by the growing aromatic olefinic peak.

Comparison of Organic Solids from Comet 81P/Wild2, Interplanetary Dust Particles, and Laboratory Synthesized Formaldehyde Polymer. The strategic collection of IDPs over the past several decades has provided us with samples of what are understood to be inorganic and organic solids derived, in part, from comets. Augmenting this collection are samples returned by the Stardust mission that are unambiguously from Comet 81P/Wild2 (32). Unfortunately, the small size (micron scale) of both IDPs and Comet 81P/Wild2 particles precludes the use of ^{13}C solid-state NMR. C-XANES microspectroscopy, afforded by synchrotron based scanning transmission X-ray microscopes (STXM), is an ideal spectroscopic method for obtaining functional group information from very small organic solid samples. C-XANES provides functional group information via absorption fine structure derived from well characterized photo-induced core level (1*s*) electronic transitions to unoccupied molecular orbitals; e.g., π^{*} and σ^{*} orbitals (33).

C-XANES analyses of IDPs (2, 34) and more recently particles recovered from Comet 81P/Wild2 reveal complex chemical structures that in many cases bear functional group similarity with primitive IOM (35–37). In addition to functional group information, combined C-, N-, and O-XANES spectra can provide elemental ratios (O/C and N/C). Analysis of a number of Comet 81P/Wild2 particles revealed considerable compositional and functional group variation with three apparent groups with one group high in O/C, another high in N/C, and a third with moderate O/C and N/C (35, 36). The C-XANES spectra of representative high O/C and moderate O/C 81P/Wild2 particles (referred to here as SD1 and SD2, respectively) reveal functional group similarity with Murchison IOM and also with the formaldehyde-derived polymer, F50 and F250 (Fig. 5). It is noted that the SD2 particle is enriched in D (38) and ^{15}N (*SI Text*) relative to terrestrial. The C-XANES spectra of each of these organic solids exhibit relatively simple spectra composed of distinct peaks at 284.8 eV (285 eV for Murchison) (olefinic/aromatic carbon), 286.5 eV (ene-ketone), and 288.5 eV (carboxyl). The similarity in these absorption spectra indicates that each organic solid contains the same types of functional groups. The variation in relative intensity (e.g., the intensity of the aromatic peak at 285 eV relative to the ene-ketone peak at 286.5 eV) indicates changes in molecular structure that may reflect transformation that took place during some type of processing; e.g., parent body processing in the case of Murchison IOM.

Comet particle SD1 is the exception in that it exhibits absorption intensity predominantly at 289.3 eV, Fig. 5*A* (SD2 also exhibits considerable absorption at this energy) consistent with a molecular structure dominated by polyalcohol moieties. Polyalcohols (e.g., carbohydrates and formaldehyde-derived sugars) are highly susceptible to H_2O elimination yielding ene-ketone moieties (at 286.5 eV), a signature feature of partially degraded polyalcohols (39). The presence of ene-ketone moieties is striking in both formaldehyde polymer samples (F50 and F250; Fig. 1*A*). The clear and significant presence of ene-ketone moieties in SD2 and Murchison IOM provides strong support for the idea that a significant portion of these extraterrestrial organic solids having originated from a polyalcohol polymer.

The chemical connection between extraterrestrial organic solids and formaldehyde-derived polymeric material is particularly apparent in the case of anhydrous IDPs, thought to be derived from comets. In Fig. 5*B* C-XANES spectra of IDPs, three

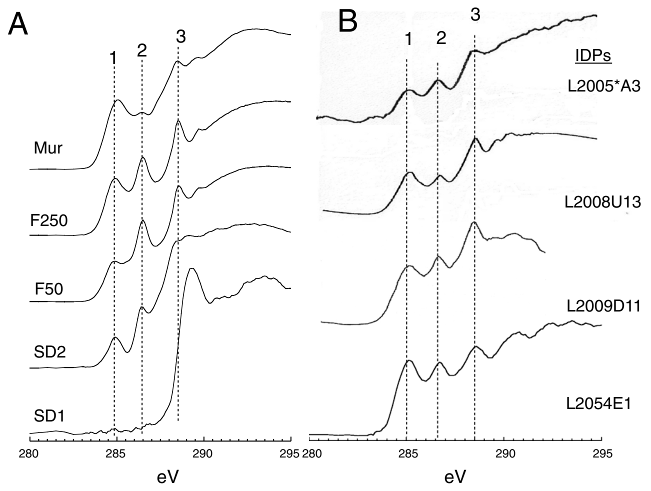

Fig. 5. (*A*) C-XANES spectra of organic matter from IOM from Murchison, a CM2 carbonaceous chondrite (**MUR**), Comet Wild2/81P [**SD1**, designation FC12, 16, 1, 10 and **SD2**, designation FC9, 13, 1, 8 (12)], and formose polymer (**F50**, as synthesized, and **F250** hydrothermally altered); spectra are offset vertically for clarity. Isotopic measurements of SD2 reveal enrichments in both D and ^{15}N ($\delta D = 900‰$; $\delta^{15}N = +70‰$) confirming the cometary origin of this grain (38). Organic solids **SD2, F50, F250** exhibit intensity at 284.8 eV (peak 1), resulting from the $1s$-π^* transition olefinic carbon, Murchison exhibits its lowest energy $1s$-π^* transition at 285.1 eV indicating the presence of both olefinic and aromatic carbon. All four of these organic solids also exhibit sharp absorption at 286.5 eV (peak 2) resulting from a $1s$-π^* transition associated with ketone group adjacent to an olefin (ene-ketone); as well as a sharp absorption at 288.5 eV (peak 3) indicating the presence of carboxyl (the weak feature near 290 eV indicates that the carboxyl moieties are immediately adjacent to double bonded carbon). Comet Wild 2/81P particle **SD1** exhibits intensity only at 289.3 eV, consistent with a dominantly polyalcohol (sugar-like) structure. (*B*) C-XANES spectra of various anhydrous IDP L2005*A3 (34), L2009D11 (40), and L2054E1(41) and one hydrous IDP L2008U13 (34). Each IDP exhibits intense absorption at 285, 286.5, and 288.5 eV, indicating that the molecular structure of the IDP's is identical at the functional group level to SD2, F50, and F250, and similar to the Murchison organic solids.

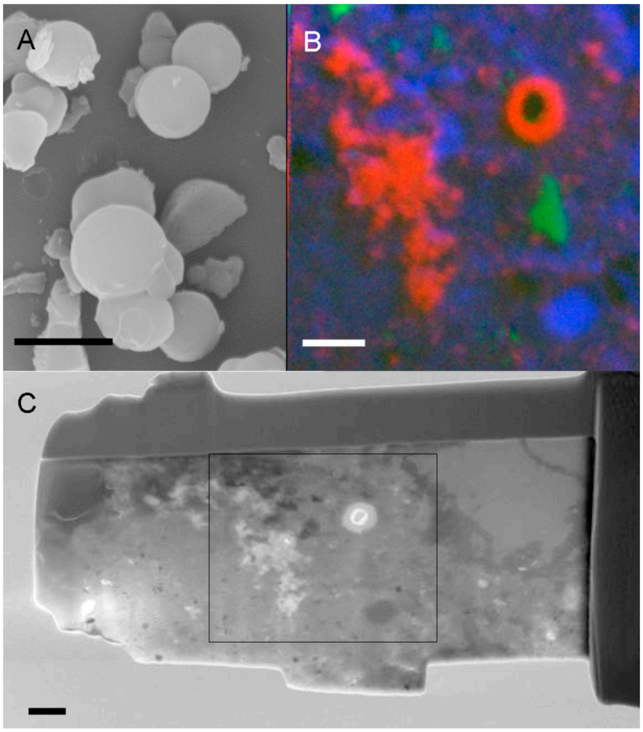

Fig. 6. (*A*) SEM images of typical organic micro- and nanospherules that spontaneously form during the formose reaction in an aqueous medium. (*B*) A Scanning transmission X-ray map of carbon (red), iron (blue), and calcium (green) concentration in a ultrathin (focused ion beam milled) section of the matrix of an type 3.0 Ordinary chondrite (QUE97008). For each 50×50 nm pixel the – log of the ratio of the transmission above to tranmission below the carbon 1*s*, calcium 2*p*, and iron 2*p* absorption edges are computed, plotted and overlayed yielding an image where the concentration of carbon, iron, and calcium are highlighted. A hollow carbonaceous nanoglobule is clearly visible. (*C*) A high-resolution scanning transmission electron microscopy bright field image of the entire FIB (5 by 10 μm) section revealing the carbonaceous nanoglobule. The scale bars in each image are 1 μm.

anhydrous (34, 40, 41) and one hydrous (34), are reproduced here for direct comparison with the organic solids in Fig. 5*A*. In terms of the functional groups present, the IDP organics are identical to the formaldehyde-derived organic solids (Fig. 5*A*); where again intense peaks are observed corresponding to olefinic carbon, ene-ketone, and carboxyl (exactly at 284.8, 286.5, and 288.5 eV, respectively). These data indicate that a clearly defined chemical relationship exists between formaldehyde polymer and organic solids in some Comet 81P/Wild2 particles, IDPs, and primitive chondritic IOM.

Formation of Microspherules. It is known that the fine-scale morphology of formaldehyde polymer is as small hollow (and some solid) microspherules (42). Similarly, some simple sugars when heated at moderate temperatures also form microspherules (43). It is, therefore, not surprising that scanning electron microscopy of the formaldehdye polymer synthesized in this study reveals an abundance of nano- and microspherules with diameters in the 100 nm to 10 μm range (Fig. 6*A*).

The formation of nano- and microspherules during formaldehyde polymerization is indicative of the formation of a microemulsion; i.e., the molecular precursor to the polymer is insoluble in water and phase separates into a second liquid phase. That the formaldehyde polymer is insoluble in water is not surprising given the molecular structure evident in Fig. 4. The observation that formaldehyde polymer forms microspherules is interesting because carbonaceous nanoglubules are ubiquitous in the matrices of chondritic meteorites (44–46) (e.g., Fig. 6*B*). In some cases chondritic nanoglobules are isotopically enriched in D and ^{15}N; which has led to the interpretation that the organic constituents of the nanoglobules were synthesized at very low temperatures (10–50 K) (45). Notwithstanding the unusual isotopic enrichments, the chondritic nanoglobules (e.g., the nanoglobule from the chondrite QUE97008 imaged in Fig. 6 *B* and *C*) are remarkably similar in shape and size to the formaldehyde polymer nanospherules (Fig. 6 *A*–*C*). This observation coupled with the clearly defined chemical similarities between the formaldehyde polymer and both chondritic and certain cometary organics may indicate that chondritic nanoglobules actually formed in a wet, low-temperature, environment.

Petrologic type 1 and 2 chondritic parent bodies have experienced extensive fluid rock interaction, thus an aqueous origin for chondritic organic nanoglobules during an early wet stage of parent body evolution does not present an intractable problem. In the case of comets in the Oort cloud and Kuiper belt, however, the ambient temperature was far below the freezing point of water, which would hinder formaldehyde polymerization let alone the formation of nanoglobules. It is possible that collisions of icy planetesimals in the Kuiper belt could yield sufficient energy to create short-lived wet regions during which condensation of cometary formaldehyde could proceed. Alternatively, it is possible that formaldehyde-derived organic solids formed originally in small warm wet bodies further within the solar system and were entrained in the outward radial transport flow at the disk midplane (16) [i.e., both low-temperature organic matter and high temperature inner solar system silicates (47)] were incorporated into the comet out in the Kuiper belt. It is also important to recognize that all samples of comets available for analysis, IDPs and Comet 81P/Wild 2, are derived from comets that have passed through the inner solar system and are, therefore, processed to at least some degree (48).

Conclusions

The data presented here show that considerable similarity exists in the molecular structure of organic solids in primitive chondritic and cometary bodies and that the origin of a significant fraction of organic solids in primitive solar system objects can logically be attributed to formaldehyde polymerization. Formaldehyde is relatively abundant in the galaxy and also in comets. The formaldehyde polymerization and subsequent reactions provide a facile route toward considerable chemical complexity under conditions of only modest temperatures; a requirement given that primitive chondritic IOM could only have formed and remained at modest temperatures. It is noted that a connection to formaldehyde polymer is evident in only two of the three apparent classes of organic particles detected in Comet 81P/Wild2 samples; the very high N/C particles (35, 36) do not exhibit any of the spectral attributes consistent with a formaldehyde polymer precursor and their origin remains undetermined. It is also noted that whereas formaldehyde polymerization may explain the origin of IOM; any relationship between such reactions and the complex suite of soluble organic matter also present in carbonaceous chondrites remains to be determined.

Materials and Methods

The ^{13}C solid-state NMR experiments were performed on a Varian–Chemagnetics Infinity 300 spectrometer employing a 7.05 T superconducting solenoid magnet. IOM was isolated from Murchison via dissolution of silicate with aqueous CsF. Formaldehyde polymer was synthesized in aqueous alkaline solutions from equimolar mixtures of formaldehyde and glycolaldehyde. C-XANES analyses were performed using the STXM located at beam line 5.3.2, the Advanced Light Source, Lawrence Berkeley Laboratory. The ordinary chondrite QUE97008 was supplied by the Meteorite Working Group and prepared for STXM analysis using a focused ion beam (FIB) microscope located at the Naval Research Laboratory (*SI Text*). The isotopic composition of one comet 81P/Wild 2 sample was measured with a Cameca NanoSIMS 50L ion microprobe at the Carnegie Institution. Experimental details are provided in *SI Text*.

ACKNOWLEDGMENTS. The Advanced Light Source is a US Department of Energy supported facility. The W. M. Keck Solid State NMR facility at the Geophysical Laboratory was supported by the W. M. Keck Foundation, the National Science Foundation, and the Carnegie Institution of Washington. We gratefully acknowledge support from National Aeronautics and Space Administration Astrobiology, Origins Program, and Stardust Analysis programs is gratefully acknowledged.

1. Alexander CMO, Fogel MF, Yabuta H, Cody GD (2007) The origin and evolution of chondrites recorded in the elemental and isotopic compositions of their macromolecular matter. *Geochim Cosmochim Acta* 71:4380–4403.
2. Keller LP, et al. (2004) The nature of molecular cloud material in interplanetary dust. *Geochim Cosmochim Acta* 68:2577–2589.
3. Greenberg JM (1998) Making a comet nucleus. *Astron Astrophys* 330:375–380.
4. Allamandola LJ, Sandford SA, Valero G (1988) Photochemical and thermal evolution of interstellar/pre-cometary ice analogs. *Icarus* 76:225–252.
5. Greenberg JM, et al. (1995) Approaching the interstellar grain organic refractory component. *Astrophys J* 455:177–180.
6. Bernstein MP, Sandford SA, Allamandola LJ, Chang S, Sharberg M (1995) Organic compounds produced by photolysis of realistic interstellar and cometary ice analogs containing methanol. *Astrophys J* 454:327–344.
7. Woods PM, Millar TJ, Herbst E, Zijlstra AA (2003) The chemistry of protoplanetary nebulae. *Astron Astrophys* 402:189–199.
8. Kwok S (2004) The synthesis of organic and inorganic compounds in evolved stars. *Nature* 430:985–991.
9. Geers VC, et al. (2007) Spatially extended polycyclic aromatic hydrocarbons in circumstellar disks around T Tauri and Herbig Ae stars. *Astron Astrophys* 476:279–289.
10. Sagan C, Khare BN (1979) Tholins-organic chemistry of interstellar grains and gas. *Nature* 277:102–107.
11. Anders E, Hayatsu R, Studier MH (1973) Organic compounds in meteorites. *Science* 182:781–790.
12. Llorca J, Casanova I (2000) Reaction between H_2, CO, and H_2S over Fe,Ni metal in the solar nebula: Experimental evidence for the formation of sulfur-bearing organic molecules and sulfides. *Meteorit Planet Sci* 35:841–848.
13. Nuth JA, Johnson NM, Manning S (2008) A self-perpetuating catalyst for the production of complex organic molecules in protostellar nebulaa, in Organic Matter in Space. *Proceedings of the 251st International Astronomical Union*, eds S Kwok and SA Sandford (Cambridge University Press, Cambridge, UK), pp 403–408.
14. Morgan WA, Feigelson ED, Wang H, Frenklach M (1991) A new mechanism for the formation of meteoritic kerogen-like material. *Science* 252:109–112.
15. Saito M, Kimura Y (2009) Origin of organic globules in meteorites: Laboratory simulation using aromatic hydrocarbons. *Astrophys J* 703:147–151.
16. Ciesla FJ (2007) Outward transport of high-temperature materials around the midplane of the Solar Nebula. *Science* 318:613–615.
17. Cody GD, et al. (2008) Organic thermometry for chondritic parent bodies. *Earth Planet Sc Lett* 272:446–455.
18. Cronin JR, Pizzarello S, Frye JS (1987) ^{13}C NMR spectroscopy of insoluble carbon of carbonaceous chondrites. *Geochim Cosmochim Acta* 51:299–303.
19. Gardinier A, et al. (2000) Solid state CP/MAS ^{13}C NMR of the insoluble organic matter of the Orgueil and Murchison meteorites: Quantitative study. *Earth Planet Sc Lett* 184:9–21.
20. Cody GD, Alexander CMO, Tera F (2002) Solid-state (^{1}H and ^{13}C) nuclear magnetic resonance spectroscopy of insoluble organic residue in the Murchison meteoritre: A self-consistent quantitative analysis. *Geochim Cosmochim Acta* 66:1851–1865.
21. Cody GD, Alexander CMO (2005) NMR studies of chemical structural variation of insoluble organic matter from different carbonaceous chondrite groups. *Geochim Cosmochim Acta* 69:1085–1097.
22. Orendt AM, et al. (1993) Measurement of chemical-shift anisotropy in coal. *Magnetic Resonance of Carbonaceous Solids*, Advances in Chemistry Series 229, eds RE Botto and Y Sanada (American Chemical Society, Washington, DC), 229, pp 419–439.
23. Gan Z (1992) High-resolution chemical shift and chemical shift anisotropy correlation in solids using slow magic angle spinning. *J Am Chem Soc* 114:8307–8309.
24. Hayatsu R, et al. (1980) Phenolic ethers in the organic polymer of the Murchison meteorite. *Science* 207:1202–1204.
25. March J (1992) *Advanced Organic Chemistry* (Wiley, New York).
26. Cooper G, et al. (2001) Carbonaceous meteorites as a source of sugar-related organic compounds for the early Earth. *Nature* 414:879–882.
27. Araya E, et al. (2002) H_2CO 6 cm emission toward IRAS 1855 + 0408. *Bul Am Astron Soc* 34:1230–1231.
28. Milam S, et al. (2006) Formaldehyde in comets C/1995 01 (Hale-Bopp), C/2002 (LINEAR), and C/2001 (NEAT): Investigating the cometary origin of H_2CO. *Astrophys J* 649:1169–1177.
29. Allamandola LH, Sandford SA, Tielens AGGM, Herbst TM (1992) Infrared spectroscopy of dense clouds in the C-H stretch region. Methanol and diamonds. *Astrophys J* 399:134–146.
30. Gibb EL, Whittet DCB, Boogert ACA, Tielens AGGM (2004) Interstellar ice: The infrared space observatory legacy. *Astrophys J* 151:35–73.
31. Shutte WA, Allamandola LJ, Sandford SA (1993) Formaldehyde and organic molecule production in astrophysical ices at cryogenic temperatures. *Science* 259:1143–1145.
32. Brownlee D, et al. (2006) Comet 81P/Wild 2 under a microscope. *Science* 314:1711–1716.
33. Stöhr J (1992) *NEXAFS Spectroscopy* (Springer, New York).
34. Flynn GJ, Keller LP, Feser M, Wirick S, Jacobsen C (2003) The origins of organic matter in the Solar System: Evidence form interplanetary dust particles. *Geochim Cosmochim Acta* 67:4791–4806.
35. Sandford SA, et al. (2006) Organics captured from comet 81P/Wild2 by the Stardust spacecraft. *Science* 314:1720–1724.
36. Cody GD, et al. (2008) Quantitative organic and light-element analysis of comet 81P/Wild2 particles using C-, N-, and O-μXANES. *Meteorit Planet Sci* 43:353–365.
37. Matrjt G, et al. (2008) Carbon investigation of two Stardust particles: A TEM, NanoSIMS, and XANES study. *Meteorit Planet Sci* 43:315–334.
38. McKeegan KD, et al. (2006) Isotopic compositions of cometary matter returned by Stardust. *Science* 314:1724–1728.
39. Cody GD, Brandes J, Jacobsen J, Wirick S (2009) Soft X-ray induced chemical modification of polysaccharides in vascular plant cell walls. *J Elect Spect Rel Phenom* 170:57–64.
40. Flynn GJ, Keller LP, Wirick S, Jacobsen J (2008) *Organic Matter in Interplanetary Dust Particles. In Organic Matter in Space*, eds S Kwok and SA Sandford (Cambridge University Press), pp 267–276.
41. Busemann H, et al. (2009) Ultra-primitive interplanetary dust particles from the comet 26P/Griggg-Skjellerup dust stream collection. *Earth Planet Sc Lett* 288:44–57.
42. Weber A (2005) Growth of organic microspherules in sugar-ammonia reactions. *Origins Life Evol B* 35:523–536.
43. Rand D, Belenky M, Herzfeld J (2010) Microspherules from sugars in the absense of nitrogen. *Orig Life Evol Biosph*, 41 pp:17–22.
44. Alpern B, Benkheiri Y (1973) Distribution de la matiére organique dans la métórite d'Orguiel par microscopy en fluorescence. *Earth Planet Sc Lett* 19:422–428.
45. Kakamura-Messenger K, Messenger S, Keller LP, Clemett S, Zolensky MJ (2006) Organic globules in the Tagish Lake meteorite: Remnants of the protoplanetary disk. *Science* 314:1439–1442.
46. Garvie LAJ, Baumgardner G, Buseck PR (2008) Scanning electron microscopical and cross-sectional analysis of extraterrestrial carbonaceous nanoglobules. *Meteorit Planet Sci* 43:899–903.
47. Zolensky ME, et al. (2006) Mineralogy and petrology of comet 81P/Wild 2 nucleus samples. *Science* 314:1735–1739.
48. Stern A (2003) The evolution of comets in the Oort cloud and Kuiper belt. *Nature* 424:639–642.